

---

# OXIDIZED MULTI-WALLED CARBON NANOTUBE FILM FABRICATION AND CHARACTERIZATION

Kastanis D.<sup>1</sup>, Tasis D.<sup>2\*</sup>, Papagelis K.<sup>2</sup>, Parthenios J.<sup>1</sup>, Tsakiroglou C.<sup>1</sup>,  
Galiotis C.<sup>1,2</sup>

<sup>1</sup>FORTH/ICE-HT, Stadiou Str., 26504 Rion Patras, Greece

<sup>2</sup>Department of Materials Science, University of Patras, 26504 Patras, Greece

\*Author to whom correspondence should be addressed  
dtassis@upatras.gr

Received 17 October 2007; accepted 30 December 2007

## ABSTRACT

The topological and mechanical properties of carbon nanotube films prepared by different oxidized treatments have been studied. Tensile parameters have been found to be strongly correlated with topological parameters such as porosity and bundle size. It was found that low porosity films prepared from highly oxidized CNTs result in the enhancement of their mechanical properties.

## 1. INTRODUCTION

The discovery of carbon nanotubes (CNTs) by Iijima in 1991 [1] has initiated a large number of scientific investigations in an attempt to explore their superb mechanical, electrical and thermal properties. Experimental studies [2,3] have shown that longitudinal elastic moduli of the order of 1TPa and tensile strengths in excess of 45 GPa can be achieved for small ropes of single-walled CNTs.

However, potential macroscale applications have been hindered as bulk nanotube material consists mainly of aggregated bundles bound together by weak van der Waals interactions. This results in a massive reduction in the bulk mechanical properties when compared to that of individual tubes. Recently, some progress has been made using a solid state process to organize CNT-containing aligned arrays into functional macroscale superstructures in the form of yarns and thin sheets [4]. In an alternative approach, researchers have fabricated self-supporting mats of entangled tubes by a solution-based protocol involving filtration of stable CNT suspension [5].

Such nanoporous preforms, the so called buckypapers, have already been proposed as reinforcements in polymer composites [6], actuators [7], catalyst supports [8] and scaffolds for biomineralization assays [9]. Concerning their structural integrity, a considerable effort has been made

into measuring the mechanical properties of species containing single-wall CNT material. Moduli and breaking strengths were reported to fall into the 1-8 GPa and 6-33 MPa range, respectively [10]. Since the mechanical properties of buckypapers are primarily determined by the tube-tube interactions, chemical functionalization of the CNT sidewalls and tips could be utilized to increase the modulus and strength of the CNT buckypapers. To our knowledge, a detailed study about the mechanical integrity and porous structure of buckypapers consisting of functionalized multi-walled CNTs (MWCNTs) has not been applied yet. In a recent study, Kukovec and co-workers [11] have studied the morphology and the gas permeability of multi-walled CNT mats by electron microscopy and gas adsorption analysis.

In this work a systematic experimental campaign has been attempted to study the effect of surface oxidation of MWCNTs on the mechanical properties- tensile modulus, strength and ductility of CNT films fabricated via vacuum filtration. Furthermore, the correlation between the pore size distribution and the homogeneity of the CNT network with each oxidation scheme is also discussed.

## 2. EXPERIMENTAL AND MATERIALS

The material used in this work was thin MWCNTs supplied by Nanocyl SA. Their average diameter was 15 nm with purity around 80% as claimed by the sup-

plier. As-received MWCNTs were further purified using concentrated hydrochloric acid (37%). MWCNTs were then oxidized using three different chemical treatments namely, ammonium hydroxide/hydrogen peroxide mixture, sulfuric acid/hydrogen peroxide (piranha) and hot nitric acid. Details for the oxidation protocols and the characterization of the treated MWCNTs have been reported previously [12].

Concerning the fabrication of MWCNT buckypapers stable aqueous CNT suspensions at a concentration of 0.125 mg/ml were prepared by tip sonication for 30 min. These dispersions were then vacuum filtered through polycarbonate membrane filters of 450 nm pore size. After drying at room temperature in a vacuum oven for 24 hours the CNT films were peeled off from the filtration membrane. The average thickness of the produced buckypapers is approximately 100  $\mu\text{m}$  and their diameter about 9 cm.

Scanning electron microscopy (SEM) was performed using a LEO SUPRA 35 VP scanning electron microscope. Mercury intrusion curves of the studied CNT sheets were obtained using a Quantachrome PoreMaster 60 Hg Porosimeter. Rectangular pieces of 10 x 30 mm were cut from all the CNT films. The capillary pressure,  $P_c$ , has been replaced by the diameter of an equivalent cylindrical tube,  $D$ , according to the relation:

$$P_c = 4\gamma \cos\theta / D \quad (1)$$

where  $\gamma$  is the surface tension of Hg ( $= 0.48 \text{ N m}^{-1}$ ) and  $\theta$  is the contact angle ( $= 40^\circ$ ). Mechanical testing was performed in a TA Instruments Dynamic Mechanical Analyzer Q800 with a displacement rate of 10  $\mu\text{m}/\text{min}$  on strips of dimensions 24 x 8 mm<sup>2</sup>. For each film type, stress-strain curves were measured for five strips.

### 3. RESULTS AND DISCUSSION

In Fig.1 a typical batch of the produced MWCNT films are presented. Regarding their morphology, the samples appeared as uniform, smooth and crack-free disks exhibiting significant structural integrity. In order to assess the structural topology of the CNT films SEM images and mercury porosimetry measurements have been obtained for each oxidation

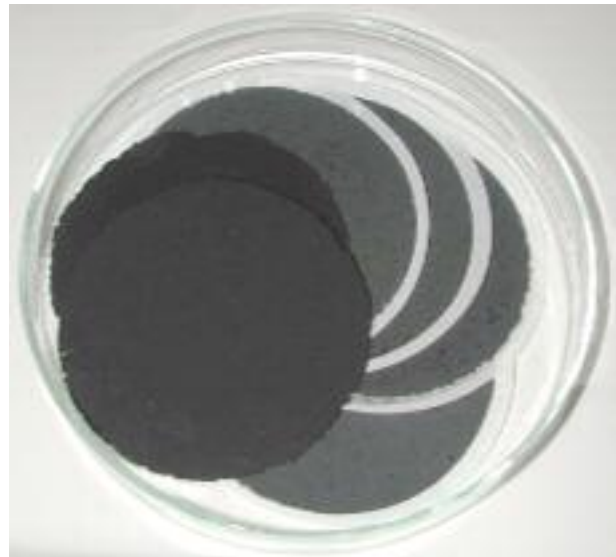
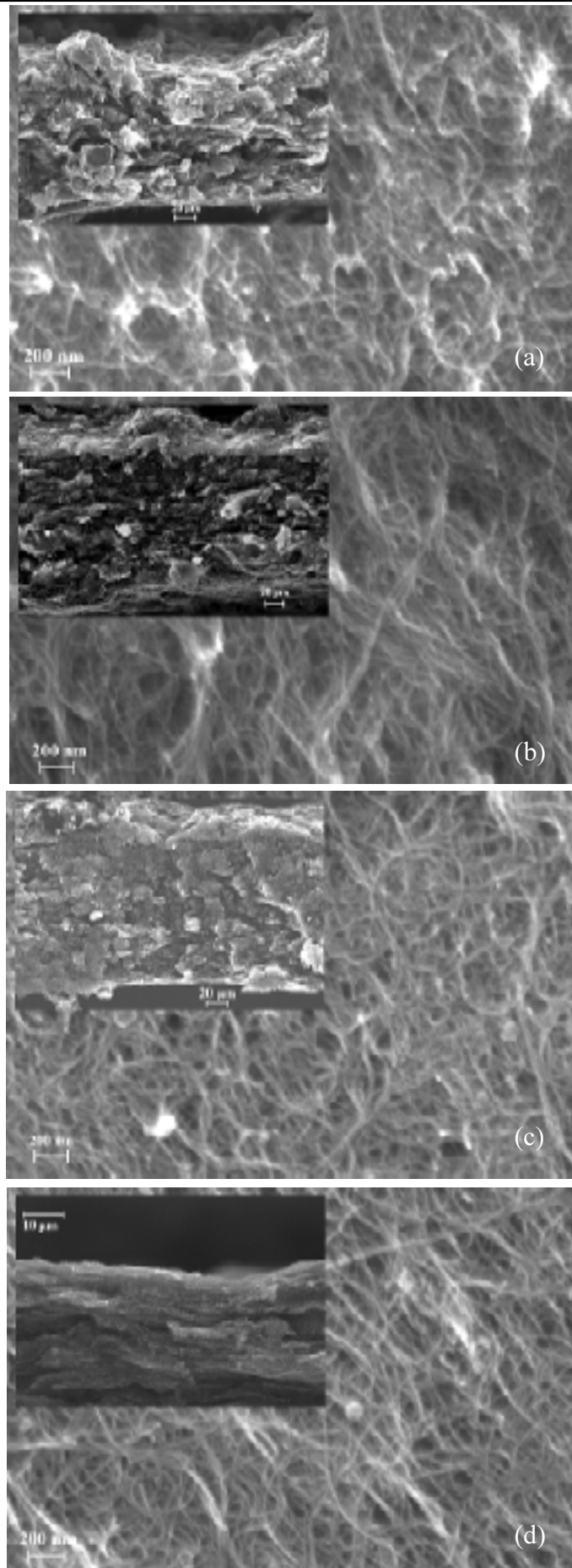


Fig. 1: A typical batch of fabricated MWCNT films.

treated sample. By comparing the top views in Fig. 2 of the presented samples, it is evident that for piranha and nitric acid-treated samples the pore structure seems to be more uniform indicating better tube dispersion in the suspension during the filtration process. This is further supported from the edge cross sectional low resolution SEM images (insets in Fig.2) where a more homogeneous and dense morphology is clearly observed. In sharp contrast, basic (ammonium hydroxide/hydrogen peroxide mixture) and HCl-treated materials are deposited as large agglomerates forming voids some of them having dimensions in the micrometer scale.

In Fig.3a the Hg intrusion curves are shown, where three different types of porosity can be clearly distinguished:

1. The surface porosity ( $D > 10 \mu\text{m}$ ) consists of large and fully accessible to Hg pores which are irregularities of the external surface of the film and are not representative of the internal porosity. Because of the small thickness of the films, surface pores comprise an important fraction of the total pore volume. The contribution fraction of surface porosity to total porosity is expected to decrease significantly as the thickness of the film increases.
2. The *inter-bundle porosity* ( $10 \mu\text{m} < D < 0.01 \mu\text{m}$ ) is the pore space left between the bundles of nano-tubes, spans a very broad range of pore



**Fig. 2:** SEM images of the surface of the fabricated MWCNT films for different treatment types: (a) HCl, (b) Ammonia, (c) piranha and (d) nitric acid treated. Inset images come from the cross section of the film.

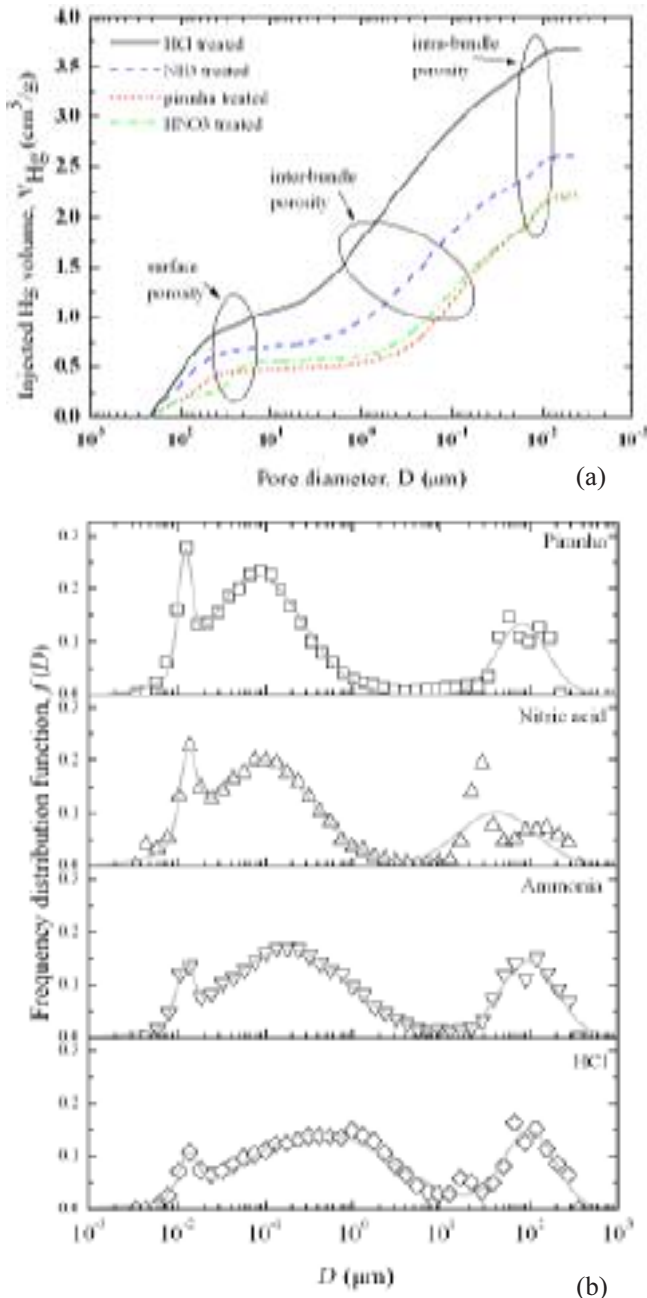


**Fig. 3:** (a) Measured Hg intrusion curves. (b) The pore diameter distributions resulting from Hg intrusion curves are compared to tri-modal fitting functions.

length scales, covering 3 to 4 orders of magnitude, (Fig.3a) and is indicative of the density and homogeneity of the network created by the nanotube bundles. This porosity is of high importance for the mechanical properties of the films.

3. The *intra-bundle porosity* ( $D < 0.01 \mu\text{m}$ ) concerns the pore networks created between the nanotubes, spans a narrow range of pore sizes (Fig.3a) and the mean pore diameter is expected to be comparable to the mean size of nanotubes.

For the complete analysis of the pore structure of such multi-scale porous materials, sophisticated methods based on the combination of the datasets from various experimental techniques (e.g. BSEM images, Hg porosimetry,  $N_2$  sorption, NMR, etc) with numerical modelling are required [13, 14, 15]. However, even a simple analysis based on the conventional model of parallel cylindrical tubes allows us to get an insight into the pore structure of films. So, the complete volume-based pore-diameter distributions were obtained by differentiating the Hg intrusion curves (Fig.3b). In order to distribute total porosity to the aforementioned sub-porosities, each pore diameter distribution was fitted with a tri-modal distribution function composed of log-normal component distribution functions. The results of the fitting are shown in Table 1 and Fig.3b.

For all films, the intra-bundle porosity has a mean pore diameter (Table 1) ranging from ~12 nm to ~15 nm, values which are comparable to the mean diameter of nanotubes. The mean value of the inter-bundle pore diameter distribution shifts to larger sizes and its width increases as one goes from piranha- to nitric acid- to Ammonia- to HCl-treated films (Table 1). The smaller the mean pore diameter, and the narrower the pore-diameter distribution of the inter-bundle porosity, the more homogeneous and denser the film. The higher density of piranha- and nitric acid-treated films, compared to Ammonia- and HCl-treated films, is reflected in the lower sum of the specific pore volumes of inter- and intra-bundle porosities ( $V_{i1} + V_{i2}$  in Table 2). On the other hand, the relatively small width of the pore diameter distribution of inter-bundle porosity for piranha- and nitric acid-treated films is associated with well-organized and homogeneous structures (Table 1).

Stress - strain curves obtained from the four samples tested are shown in Fig. 4. Numerical values of Young's moduli, tensile and breaking strength are presented in Table 3. By comparing the mechanical parameters of each film type, the nitric acid and piranha treated nanotube films exhibit the highest mechanical properties.

It is expected that the colloidal stability of the aqueous suspensions would affect considerably the CNTs stacking motif and degree of homogeneity within the

**Table 1:** Mean value ( $\mu$ ), standard deviation ( $\sigma$ ) and contribution fraction ( $c_i$ ) of the log-normal component of pore-diameter distribution ( $i=1, 2, 3$  for surface, inter-bundle, and intra-bundle porosity, respectively).

Film type	$c_1$	$\mu_1$ ( $\mu\text{m}$ )	$\sigma_1$ ( $\mu\text{m}$ )	$c_2$	$\mu_2$ ( $\mu\text{m}$ )	$\sigma_2$ ( $\mu\text{m}$ )	$c_3$	$\mu_3$ ( $\mu\text{m}$ )	$\sigma_3$ ( $\mu\text{m}$ )
MWCNT- Piranha	0.222	102.5	75.26	0.682	0.167	0.303	0.096	0.0127	0.0023
MWCNT -Nitric	0.257	70.74	93.84	0.660	0.224	0.504	0.083	0.0138	0.0030
MWCNT- Ammonia	0.272	128.9	111.8	0.669	0.641	2.177	0.059	0.0127	0.0029
MWCNT -HCl	0.245	125.3	93.64	0.708	2.714	17.95	0.047	0.0139	0.0035

**Table 2:** Pore volume distribution of films corresponding to surface, inter-bundle and intra-bundle porosity.

Film type	Total pore volume, $V_p$ ( $\text{cm}^3/\text{g}$ )	Surface pore volume ( $V_s=c_1V_p$ ) ( $\text{cm}^3/\text{g}$ )	Inter-bundle pore volume ( $V_{i1}=c_2V_p$ ) ( $\text{cm}^3/\text{g}$ )	Intra-bundle pore volume ( $V_{i2}=c_3V_p$ ) ( $\text{cm}^3/\text{g}$ )
MWCNT- Piranha	2.213	0.491	1.509	0.212
MWCNT -Nitric	2.207	0.566	1.456	0.184
MWCNT - Ammonia	2.607	0.708	1.744	0.154
MWCNT -HCl	3.675	0.901	2.602	0.171

**Table 3:** Tensile parameters of oxidized MWCNT films.

Film type	Young Modulus (MPa)	Strength (MPa)	Ductility (%)
MWCNT -HCl	$57 \pm 3$	$0.4 \pm 0.1$	$0.6 \pm 0.1$
MWCNT -Ammonia	$62 \pm 7$	$1.1 \pm 0.1$	$1 \pm 0.2$
MWCNT- Piranha	$214 \pm 67$	$2.4 \pm 0.3$	$1.2 \pm 0.2$
MWCNT -Nitric	$448 \pm 44$	$2.6 \pm 0.2$	$0.8 \pm 0.1$

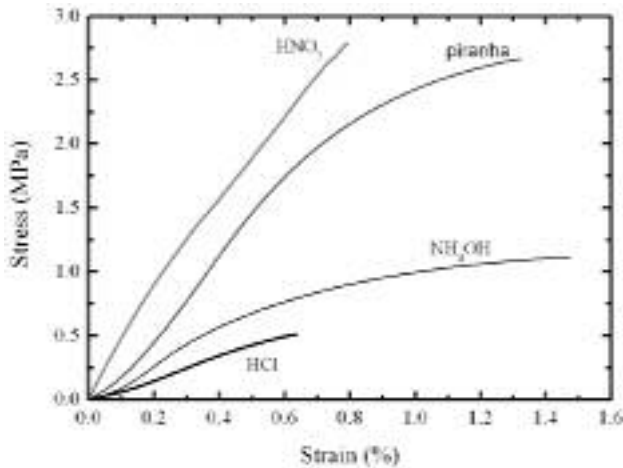


**Fig. 4:** Representative stress-strain curves for fabricated MWCNT films.

buckypaper and consequently stress transfer efficiency [16,17]. Thus, filtration of heavily oxidized (nitric acid and piranha treatments) CNT suspensions forms a homogeneous mat of randomly interconnected isolated tubes. This is in agreement with the inter-bundle pore volume,  $V_{i1}$ , values (Table 2), where lower porosity corresponds to films with higher oxygen content.

On the other hand, there is a clear correlation between the inter-bundle network porosity and the tensile parameters of the film. While the nitric acid treated films exhibit the highest Young's modulus and strength, its porosity is the minimum one. This can be explained by the efficient packing of individually deposited tubes during the filtration process, leading to enhanced stress transfer due to a higher density of inter-tube junctions.

**4. CONCLUSIONS**

By increasing the density of carboxylic and hydroxylic group on the CNT surface, high quality dispersions and low porosity buckypaper films are produced. It is observed that low porosity films from highly oxidized CNTs result in the enhancement of their mechanical properties. These films can be ideal candidates as structural materials for fabrication high CNT volume fraction nanocomposites.

**ACKNOWLEDGEMENTS**

Financial support from the Marie Curie Transfer of Knowledge program CNTCOMP [Contract No.: MTKD-CT-2005-029876] is gratefully acknowledged.

References:

1. Iijima, S., "Helical microtubules of graphitic carbon", *Nature*, **354** (1991), 354-356.
2. Salvetat, J. P., Briggs, G.A.D., Bonard, J.-M., Bacsá, R.R., Kulik, A.J., Stoeckli, T., Burnham, N.A., Forroo, L., "Elastic and Shear Moduli of Single-Walled Carbon Nanotube Ropes", *Physical Review Letters*, **82** (1999), 944-947.
3. Walters, D.A., Ericson, L.M., Casavant, M.J., Liu, J., Colbert, D.T., Smith, K.A., Smalley, R.E., "Elastic strain of freely suspended single-wall carbon nanotube ropes", *Applied Physics Letters*, **74** (1999), 3803-3805.
4. Atkinson K. R., Hawkins, S. C., Huynh, C., Skourtis C., Dai, J., Zhang, M., Fang, S., Zakhidov, A. A., Lee, S. B., Aliev, A. E., Williams, C. D., Baughman, R. H., "Multifunctional carbon nanotube yarns and transparent sheets: Fabrication, properties, and applications", *Physica B*, **394** (2007), 339-343.
5. Gou, J., Liang, Z., Wang, B., "Experimental Design and Optimization of Dispersion process for single-walled carbon nanotube buckypaper", *International Journal of Nanoscience*, **3** (2004), 293-307.
6. Wang, Z., Liang Z., Wang B., Zhang C., Kramer L., "Processing and property investigation of single-walled carbon nanotube (SWNT) buckypaper/epoxy resin matrix nanocomposites", *Composites: Part A*, **35** (2004), 1225-1232.
7. Vohrer, U., Kolaric, I., Haque, M.H., Roth, S., Detlaff-Weglikowska, U., "Carbon nanotube sheets for the use as artificial muscles", *Carbon*, **42** (2004), 1159-1164.
8. Munoz, E., Dalton, A.B., Collins, S., Zakhidov, A.A., Baughman, R.H., Zhou, W.L., He, J., O'Connor, C. J., McCarthy, B., Blau, W. J., "Synthesis of SiC nanorods from sheets of single-walled carbon nanotubes", *Chemical Physics Letters*, **359** (2002), 397-402.
9. Tasis, D., Kastanis, D., Galiotis, C., Bouropoulos, N., "Growth of calcium phosphate mineral on carbon nanotube buckypapers", *Physica Status Solidi (b)*, **243** (2006), 3230 - 3233.
10. Berhan, L., Yi, Y. B., Sastry, A. M., Munoz, E., Selvidge, M., Baughman, R., "Mechanical properties of nanotube sheets: Alterations in joint morphology and achievable moduli in manufacturable materials", *Journal of Applied Physics*, **95** (2004), 4335-4345.
11. Smajda, R., Kukovec, A., Konya, Z., Kiricsi, I., "Structure and gas permeability of multi-wall carbon nanotube buckypapers", *Carbon*, **45** (2007), 1176-1184.
12. Datsyuk, V., Kalyva, M., Papagelis, K., Parthenios, J., Tasis, D., Siokou, A., Kallitsis, I., Galiotis, C., "Chemical Oxidation of Multi Walled Carbon Nanotubes", *Carbon*, (2007) (to be published)
13. Padhy, G. S., Lemaire, C., Amirtharaj, E.S., Ioannidis, M.A. "Pore size distribution in multiscale porous media as revealed by DDIF-NMR, mercury porosimetry and statistical image analysis", *Colloids and Surfaces A: Physicochemical and Engineering Aspects*, **300** (2007), 222-234.
14. Tsakiroglou, C.D., Burganos, V. N., Jacobsen, J., "Pore structure analysis by using nitrogen sorption and mercury intrusion data", *AIChE J.*, **50** (2004) 489-510.
15. Tsakiroglou, C. D., Ioannidis, M. A., "Dual porosity modelling of the pore structure and transport properties of a contaminated soil", *Eur. J. Soil Sci.*, in press (2008).
16. Guild, F. J., Vlatts C., Galiotis, C., "Modelling of Stress Transfer in Fiber Composites", *Composites Science and Technology*, **50** (1994), 319-332.
17. Chohan, V., Galiotis, C., "Effects of interface, volume fraction and geometry on stress redistribution in polymer composites under tension", *Composites Science and Technology*, **8** (1997), 1089-1101.